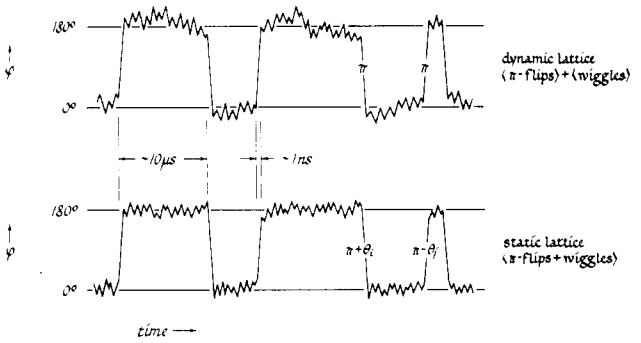

Figure 7. Angular excursions for polycarbonate rings under two assumptions for the combination of 180° flips and small-amplitude wiggles. The time for an individual flip may be as short as 1 ps. Many flips can therefore occur in a fraction of a nanosecond. (Only single flips are shown in the figure.) While the total of all elapsed time a ring spends in flipping is small (as established by the experimental dipolar tensors), the time between episodes of flipping must still be short compared to the inverse of C–H dipolar coupling.

the inherent mobility of isolated rings, the constraints produced by packing in the glass, and the cooperative lattice distortion which allows large-amplitude ring motion. We have not attempted an *explanation* of the ring-flip mechanism in terms of activation volumes or monomer-packing symmetry. This requires new experiments to measure directly the motional correlations of rings and, more importantly, a new understanding of the packing interactions in the glass, a development which we feel must await advances in computer modeling of the disordered solid state.

Nevertheless, we can speculate that the presence in PC of a high degree of cooperativity between and along chains in 100-kHz large-amplitude microscopic molecular motions and the unusually high impact strength of PC (its ability to respond to sudden and intense local strains) is no accident. Although impact strength relies ultimately upon irreversible deformations which we do not measure by either NMR or mechanical loss spectroscopy, if a glass has the ability to respond quickly by the cooperative motion of several chains, it seems reasonable to suppose that many chains can move together in a macroscopic response. Naturally, other factors may intervene and some polymers which show no cooperative motions under low-strain conditions may still respond under high-strain fields.

Acknowledgment. This work was supported in part by grants from the National Science Foundation Polymers Program and the Petroleum Research Fund, administered by the American Chemical Society.

Registry No. PPO (SRU), 24938-67-8; PC (SRU), 24936-68-3; PPO (polymer), 25134-01-4; PC (polymer), 25037-45-0.

References and Notes

(1) Spiess, H. W. *Colloid Polym. Sci.* **1983**, *261*, 193.
(2) Inglefield, P. T.; Amici, R. M.; Hung, C.-C.; O'Gara, J. F.; Jones, A. A. *Macromolecules* **1983**, *16*, 1552.
(3) Schaefer, J.; Stejskal, E. O.; McKay, R. A.; Dixon, W. T. *Macromolecules* **1984**, *17*, 1479.
(4) Schaefer, J.; McKay, R. A.; Stejskal, E. O.; Dixon, W. T. *J. Magn. Reson.* **1983**, *52*, 123.
(5) Hester, R. K.; Ackerman, J. L.; Neff, B. L.; Waugh, J. S. *Phys. Rev. Lett.* **1976**, *36*, 1081.
(6) Stoll, M. E.; Vega, A. J.; Vaughan, R. W. *J. Chem. Phys.* **1976**, *65*, 4093.
(7) Munowitz, M. G.; Griffin, R. G. *J. Chem. Phys.* **1982**, *76*, 2848.
(8) Herzfeld, J.; Berger, A. E. *J. Chem. Phys.* **1980**, *73*, 6021.
(9) Berne, B. J.; Pechukas, P. *J. Chem. Phys.* **1971**, *56*, 4213.
(10) Yee, A. F. *Polym. Eng. Sci.* **1977**, *17*, 213.
(11) Yee, A. F.; Smith, S. A. *Macromolecules* **1981**, *14*, 54.
(12) Bubeck, R. A.; Bales, S. E.; Smith, P. *Bull. Am. Phys. Soc.* **1984**, *29*, JT8.
(13) Tonelli, A. E. *Macromolecules* **1972**, *5*, 558.
(14) Flory, P. J. *Macromol. Chem.* **1973**, *8*, 1.
(15) Flick, J. R.; Petrie, S. E. B. *Bull. Am. Phys. Soc.* **1974**, *19*, 238.
(16) Yee, A. F. *Ann. N.Y. Acad. Sci.* **1981**, *371*, 341.
(17) Jones, A. A., O'Gara, J. F.; Inglefield, P. T.; Bendler, J. T.; Yee, A. F.; Ngai, K. L. *Macromolecules* **1983**, *16*, 658.
(18) McCammon, J. A.; Lee, C. Y.; Northrup, S. H. *J. Am. Chem. Soc.* **1983**, *105*, 2232.

Influence of Polydispersity on Polymer Self-Diffusion Measurements by Pulsed Field Gradient Nuclear Magnetic Resonance

P. T. Callaghan* and D. N. Pinder

Department of Physics and Biophysics, Massey University, Palmerston North, New Zealand. *Received June 22, 1984*

ABSTRACT: The effects of finite polymer polydispersity on the pulsed field gradient nuclear magnetic resonance (PFGNMR) measurement of polymer self-diffusion coefficients is considered both theoretically and experimentally. It is found that polystyrene solutions characterized by a polydispersity $M_w/M_n < 1.10$ present little difficulty in the interpretation of PFGNMR data. Single-exponential echo decays are observed down to attenuations in excess of 0.05 and the ensemble self-diffusion coefficient obtained lies between M_n and M_w. Polymer blends have been studied and the use of deuterated polystyrene has enabled determination of the component self-diffusion coefficients. We observe considerable microscopic averaging of molecular diffusion rates, with the greatest perturbation being suffered by the higher molar mass components. An investigation of the relative importance of reptation and tube renewal as relaxation mechanisms for random coil polymers in semidilute solution reveals that tube renewal is a weak process.

Introduction

In all experiments dealing with polymer dynamics the influence of finite polydispersity presents a conundrum. In some cases discrepancies are attributed to small polydispersity effects ($M_w/M_n < 1.10$), while in others theories are supported by data obtained where molar mass variations are larger by 1 order of magnitude. A notable example of this is the classic self-diffusion study of Klein[1] in which the reptative scaling law $D \sim M^{-2}$ was exhibited in polyethylene melts whose M_w/M_n ratios ranged between 1.8 and 3.4.

We have used pulsed field gradient nuclear magnetic resonance (PFGNMR) to measure polymer self-diffusion. It has been recently suggested by von Meerwall[2] on theo-

0024-9297/85/2218-0373$01.50/0

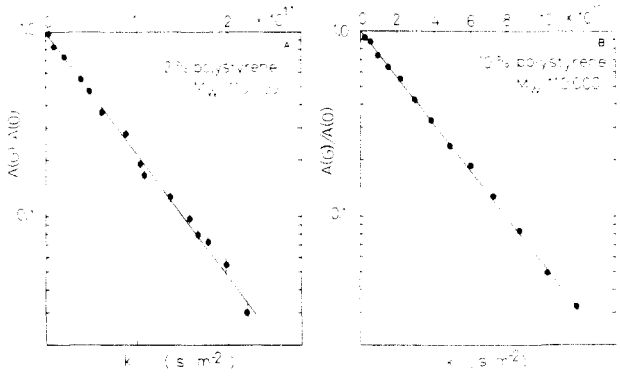

Figure 1. (A) Proton spin-echo attenuation plot for 2.0% polystyrene (M_w = 110000, M_w/M_n = 1.06) in CCl_4 at 28 °C. The straight line through the data is a linear least-squares fit yielding a single self-diffusion coefficient as given in Table II. (B) As for part A but for 10.0% polystyrene solution.

Table I
Polystyrenes Used in This Work

batch	M_w	M_w/M_n
4b	110 000[a]	<1.06
50124	233 000[a]	<1.06
	207 000[b]	<1.12

[a] Polystyrene samples supplied by Pressure Chemical Co. [b] Perdeuteriopolystyrene samples supplied by Polymer Laboratories Ltd. with M_0 = 196000 daltons.

retical grounds that even quite small polydispersities lead to a non-Gaussian dependence of the spin-echo attenuation, $A(G)/A(0)$, on the field gradient magnitude, G.

For a single molecular species with self-diffusion coefficient D_s it may be shown[3] that for field gradient pulses of magnitude G, duration δ, and separation Δ

$$\ln [A(G)/A(0)] = -kD_s \tag{1a}$$

where

$$k = \gamma^2 G^2 \delta^2 (\Delta - \delta/3) \tag{1b}$$

In all our experiments on single species polystyrene ($M_w/M_n < 1.10$) we in fact observe a linear echo decay in accordance with eq 1. Figure 1 illustrates this behavior for 2.0% 110000 molar mass polystyrene (see Table I) in carbon tetrachloride where the echo amplitude is apparently a single-exponential function down to an attenuation of order 0.05. The same linearity in the semilogarithmic plot is apparent for higher concentration samples despite the fact that the self-diffusion coefficient depends even more strongly on molar mass in this entangled regime. Further, we have performed PFGNMR experiments on dextran[4] with considerably greater polydispersity and found spin-echo semilogarithmic plots approximately linear despite large M_w/M_n ratios. In that work we were led to propose ensemble averaging.

In this paper we consider the nature of the averaging process which governs the net echo attenuation in the PFGNMR experiment. Following Bernard and Noolandi[5] we distinguish two separate aspects of the effects of polydispersity on the dynamics of polymers. The first concerns the averaging over the molecular weight distribution when a macroscopic quantity is determined by the combined properties of the individual chains comprising the distribution. In our experiment the macroscopic quantity is the net nuclear spin echo which is formed as a sum of echoes from nuclei residing on all the polymer chains. We call this averaging "macroscopic". The second aspect concerns the individual chain behavior and in particular

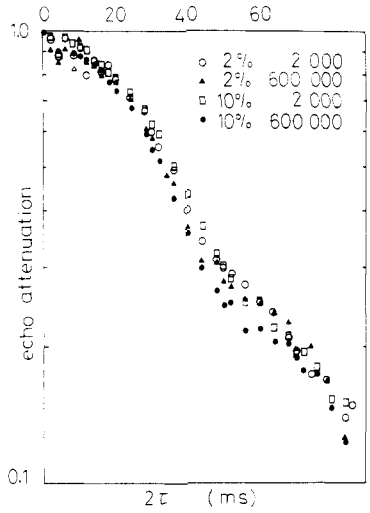

Figure 2. Benzene ring proton spin-echo amplitude vs. echo time 2τ for polystyrenes of different molar mass and at different concentrations in CCl_4 at 28 °C. It is apparent that T_2 is largely independent of molar mass and concentration for the polymer systems studied here. The modulation of the echo amplitude arises from spin–spin scalar coupling.

how the motion of one chain is influenced by the molar masses of its neighbors. This influence on the diffusive motion of the chains we term "microscopic" averaging.

We may treat these aspects in turn. If we take the first alone, we presume that each polymer of molar mass M in the polydisperse mixture has a self-diffusion coefficient identical with that which would prevail if the ensemble were monodisperse with molar mass M. In practice we might expect this assumption would be valid in the special case of infinite dilution.

Macroscopic Averaging in the PFGNMR Experiment

In the NMR experiment one might expect the relative statistical weight to each polymer coil to be determined by the number of nuclear spins it possesses and also by the decay due to transverse relaxation given by $\exp(-2\tau/T_2)$, where 2τ is the time lapse between the first rf pulse and the center of the echo. In fact, the relaxation effect is not manifest, because the molar mass and concentration dependence of T_2 is insignificant. Figure 2 shows the dependence of the spin-echo amplitude on time 2τ for the benzene ring protons of polystyrene in CCl_4 at different concentrations and molar masses. This very weak dependence of T_2 is to be expected because local segmental reorientation is the dominant spin relaxation mechanism.

We are therefore led to the simple molar mass weighted expression

$$\langle A(G)/A(0) \rangle = \int_0^\infty M \exp[-kD_s(M)] n(M)\, dM / \int_0^\infty M n(M)\, dM \tag{2}$$

where $n(M)$ is the appropriate number distribution for the polymer mixture. For a discrete blend of sharp fractions each of molar mass M and number n we write

$$\langle A(G)/A(0) \rangle = \sum_i M_i \exp(-kD_s(M_i) n_i / \sum_i M_i n_i \tag{3}$$

where $D_s(M_i)$ is the self-diffusion coefficient of those polymer coils with molar mass M_i in this particular solution. A similar interpretation applies to the distribution $D_s(M)$ in eq 2. The values of $D_s(M_i)$ [and $D_s(M)$] are not available. The macroscopic averaging assumption is that the $D_s(M)$ may be identified with those values obtained for monodisperse solutions of the same concentration.

Consider some mass M_0 used to characterize a polymer mass distribution. M_0 might for example be the weight-averaged molar mass, M_w. Bernard and Noolandi show that if the physical quantity $Q(M)$ is governed by a scaling law, $Q(M) \sim M^\alpha$, then the averaged value $\langle Q(M) \rangle$ will scale similarly with M_0, but with a numerical prefactor depending on the polydispersity, namely

$$\langle Q(M) \rangle = g(P,\alpha) M_0^\alpha \tag{4}$$

where $P = M_w/M_n$. It is interesting to note that according to this simple picture it is not the degree of polydispersity but variations in polydispersity with molar mass which perturb molar mass scaling relations.

In some experiments the physical quantity of interest cannot be averaged quite so directly. For example, in both forced Rayleigh scattering and PFGNMR, the self-diffusion coefficient is derived from an exponential decay in the signal. The average of eq 4 applies only to the leading linear term in the expansion. In general, nonlinearities will arise from polydispersity effects and it is of interest to characterize these. To do so we must choose an appropriate number distribution for the polymer fraction. In this paper we deal both with discrete blends of sharp fractions and with continuous distributions arising from the specific polymerization process appropriate to the manufacture of the polymer.

Macroscopic averaging in the discrete case may be simply treated by using eq 3. It is however useful to deal analytically with the continuous distribution. Here we follow other workers in choosing the log normal distribution which gives a good description in anionically polymerized polymers.[6] We may write the normalized distribution

$$n(M) = (\pi\sigma^2)^{-1/2} M^{-1} \exp[-\ln^2 (M/M_0)/\sigma^2] \tag{5}$$

which is derived from the normal distribution function by using the logarithm of the molar mass as the independent variable. ln (M_0) is the mode of ln (M). For brevity we write $L = \ln (M)$ and $L_0 = \ln (M_0)$.

Consider first the number-averaged and weight-averaged molar masses.

$$M_n = \int_0^\infty Mn(M)\, dM \tag{6a}$$

$$= M_0 \exp(\sigma^2/4) \tag{6b}$$

$$M_w = \int_0^\infty M^2 n(M)\, dM / \int_0^\infty Mn(M)\, dM \tag{7a}$$

$$= M_0 \exp(3\sigma^2/4) \tag{7b}$$

We will allow a scaling relation $D_s(M) = aM^\alpha$. This will apply both at extreme dilution (where $\alpha = -0.6$) and in semidilute solutions (where $\alpha = -2$). Equation 3 therefore gives

$$\langle A(G)/A(0) \rangle = (\pi\sigma^2)^{-1/2} \int_{-\infty}^\infty \exp(L) \exp(-kae^{L\alpha}) \exp(-(L - L_0)^2/\sigma^2)\, dL$$

$$= 1 - kD_1 + k^2D_2^2 - k^3D_3^3 + \ldots \tag{8}$$

where

$$D_n = D_s(M_0) \exp[\alpha(n\alpha + 2)\sigma^2/4] \tag{9}$$

D_1 corresponds to the mass-averaged diffusion coefficient and is related to $D_s(M_w)$ by

$$D_1 = D_s(M_w) \exp[(\alpha(\alpha + 2) - 3\alpha)\sigma^2/4] \tag{10}$$

The coefficient of $D_s(M_w)$ is the factor $g(P,\alpha)$ in the Bernard and Noolandi formulation of the macroscopic average (eq 4). We note that for $M_w/M_n = 1.06$ (a typical polydispersity for commercially available polystyrene sharp fractions) $g(P,\alpha)$ takes values of 1.03 and 1.19, respectively, for dilute solutions ($\alpha = -0.6$) and semidilute solutions ($\alpha = -2$).

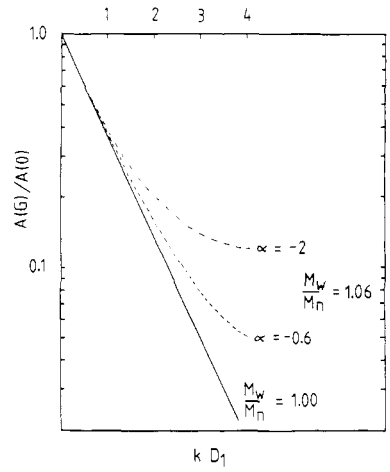

Figure 3. Calculated spin-echo attenuation plots for monodisperse and polydisperse polymer solutions using the model represented by eq 8. A log normal molar mass distribution has been assumed for the polydisperse case with $M_w/M_n = 1.06$. These calculated curves should be contrasted with the linear behavior of the data evident in Figure 1A,B.

Equations 8 and 9 enable a calculation of the shape of the echo attenuation plot allowing for macroscopic averaging alone in which case the values assumed for $D_s(M_i)$ are empirically determined from measurements on monodisperse solutions. In Figure 3 we show calculated echo attenuation plots for $M_w/M_n = 1.06$ and $\alpha = -0.6$ and -2. Even for such small polydispersity, dramatic curvature is evident, where echo attenuations down to 0.05 are employed. This calculation is consistent with the predictions of von Meerwall. In contrast the data for 110 000-dalton polystyrene ($M_w/M_n = 1.06$) in CCl_4, in both the dilute and semidilute regimes (Figure 1), are without significant curvature on this scale and indeed appear quite linear. This linearity corresponds to a much narrower range of diffusion coefficients than that predicted by the model allowing for independent molecular motion and a knowledge of the polymer mass distribution. It is possible that this discrepancy could arise from our choice of the log normal distribution which possesses a significant tail at high molar masses. However, the log normal distribution is physically realistic for this system. Consequently, we propose that the observed narrowing of the range of diffusion coefficients possessed by the polymer ensemble is predominantly due to ensemble averaging on the microscopic scale.

Microscopic Averaging

We now abandon the identification of $D_s(M_i)$ with values pertaining to monodisperse solution. The phenomenon of microscopic averaging has not been considered in previous investigations of the polydispersity effect on the measurement of self-diffusion coefficients by PFGNMR. Consequently, we introduce the concept through consideration of a simple low molecular weight binary solution.

Figure 4A shows echo attenuation graphs for benzene and butanol in binary solution.[7] Also shown are those pertaining to pure benzene and pure butanol. The independent components of the binary solution may be observed because the chemical shift in the proton NMR signal enables the benzene and butanol signals to be re-

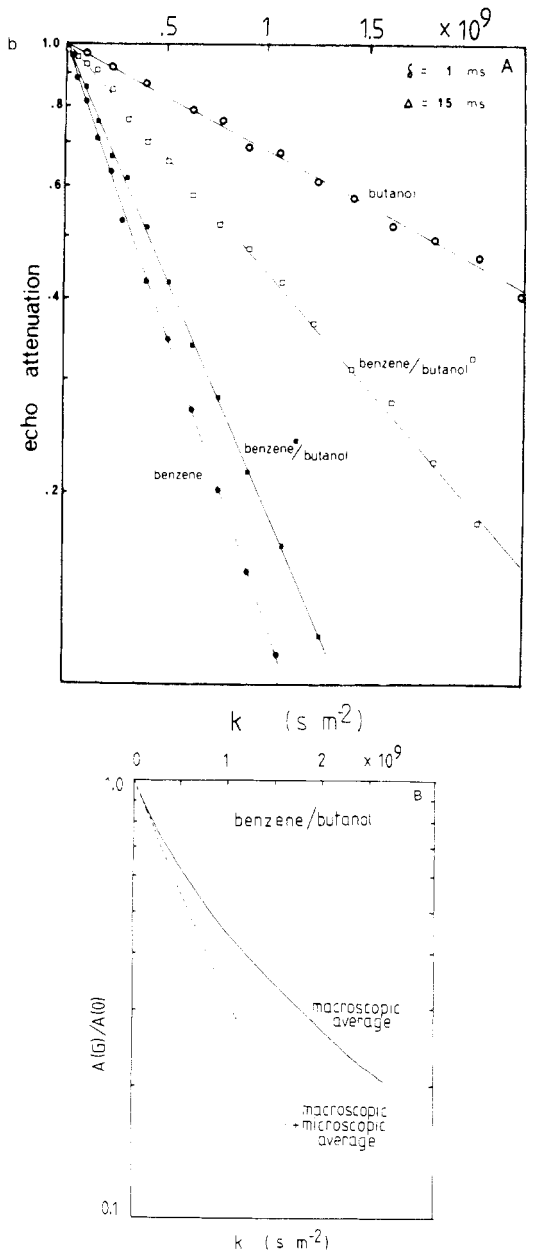

Figure 4. (A) Spin-echo attenuation plots for pure benzene and pure 1-butanol along with the component data in an equimolar mixture. The benzene and butanol proton NMR signals were resolved by means of the chemical shift. (B) Calculated spin-echo attenuation plots pertaining to the equimolar data of part A but for the case that the component NMR signals cannot be resolved and a summed echo is observed from the butanol and benzene protons. The data are no longer single exponential. The curve labeled "macroscopic average" uses diffusion coefficients for pure benzene and butanol whereas the microscopic average curve uses the actual component self-diffusion coefficients (of part A) found in the equimolar solution.

solved. Notice the self-diffusion coefficient of each binary component has approached a mean value due to the effect of microscopic averaging only. In an experiment in which the signal could not be resolved into two separately identifiable components a single curved echo attenuation plot would result as shown in Figure 4B. This latter effect corresponds to both microscopic and macroscopic averaging. Also shown in Figure 4B is the computed net echo attenuation in the absence of any averaging on the microscopic scale but including macroscopic averaging only. It is clear that microscopic averaging greatly reduces the nonlinearity in the semilogarithmic spin-echo attenuation plot, by causing the binary solution constituents to assume diffusion coefficients other than those pertaining to the pure solvents.

Consider how microscopic averaging arises. For dilute polymer solutions the diffusive motion of the coil of mass M_1 depends on both the frequency of collision with its neighbors and the perturbation to its motion subsequent to that collision. Suppose that the neighbors are a single species of mass M_2. The collision cross section and the collision perturbation depend on both M_1 and M_2. Consequently, the dilute solution is difficult to treat. By contrast the semidilute reptation model clearly distinguishes the influence of the self- and matrix-chain masses. Here

$$D_s \sim R_1^2[a/T_r + b/\theta_r] \tag{11a}$$

where T_r is the self-chain reptation time and θ_r is the relaxation time for tube reorganization, the so-called tube renewal process. The constants a and b reflect the relative importance on reptation and tube renewal in chain relaxation. Since both T_r and θ_r are governed by reptation of their respective chains

$$D_s \sim R_1^2[aM_1^{-3} + bM_2^{-3}] \tag{11b}$$

Tube renewal is the weaker process ($b < a$) and we would expect, given its dependence on M_2, the the greatest perturbation would result for chains M_1 where the matrix consisted of chains of lesser molar mass $M_2 < M_1$.

While the macroscopic averaging appropriate to the PFGNMR experiment is therefore clearly defined, the ensemble averaging occurring at a microscopic level is a matter of conjecture and the experiments reported here specifically relate to this latter phenomenon. To elucidate the change in the self-diffusion of a polymer species consequent to a change in molar mass of its neighbors, we compare the self-diffusion of a sharp fraction of molar mass M_1 with that which results when the fraction coexists in a bimodal blend with a fraction of mass M_2 differing by a factor of 2. The experiment is akin to that illustrated for benzene and butanol in Figure 4 except that the chemical shift is unavailable for the resolution of the different molar mass species and selective deuteration is employed instead.

Experimental Section

Details of our PFGNMR apparatus have been extensively reported elsewhere. Polystyrene fractions are as indicated in Table I. Spectroscopic-grade carbon tetrachloride was used and solutions were thoroughly mixed and sealed in 5-mm NMR tubes, being subsequently allowed to equilibrate for several days. All experiments were performed at 28 °C and in each case we observed center of mass motion obeying the relation

$$\langle r^2 \rangle = 6Dt \tag{12}$$

This was tested by changing the experimental time scale Δ and noting that the echo attenuation depended on the common parameter $\gamma^2G^2\delta^2(\Delta - \delta/3)$ as required by eq 1.

Bimodal Distributions

Bimodal distributions of equal numbers (equimolar) sharp fractions 110 000/233 000 molar masses were prepared in both the dilute regime (2.0%) and semidilute regime (10.0%). These mixtures are treated according to eq 3, in which the number distribution is treated as two δ functions centered on 110 000 and 233 000 molar mass, respectively. In fact, because of the small but finite polydispersity of the components the distribution is more continuous as indicated in Figure 5A and a more exact treatment would incorporate this feature. However, in view of the observed insignificance of the component polydispersity as indicated earlier in this paper we justify the

Table II
Self-Diffusion Coefficients

soln compn	concn, %	$10^{12}D_s$, m^2 s^{-1} single component	two components: known component	two components: fitted component
110 000 only	2.0	15.7 (3)		
110 000 only	10.0	2.80 (5)		
233 000 only	2.0	7.4 (1)		
233 000 only	10.0	0.71 (1)		
equimolar 110 000 + 207 000 (perdeut)	2.0	14.4 (4)		
equimolar 110 000 + 207 000 (perdeut)	10.0	2.43 (9)		
equimolar 110 000 + 233 000	2.0	10.8 (2)[a]	14.4 (4) (110 000)	10.5 (2) (233 000)[b]
equimolar 110 000 + 233 000	10.0	1.07 (1)[a]	2.43 (9) (110 000)	0.94 (3) (233 000)[c]

[a] Single-exponential forced fit. [b] 233 000 component calculated by fitting. Implied b/a ratios 1 and 0.37. [c] 233 000 component calculated by fitting. Implied b/a ratios 0.26 and 0.22.

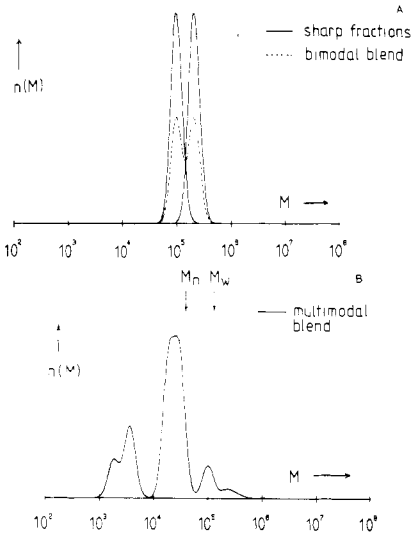

Figure 5. (A) Calculated (log normal) number distributions for polymers with M_w values of 110 000 and 233 000 and M_w/M_n = 1.06. Curves for both the sharp fractions and the equimolar blends are shown. (B) Calculated number distribution for the polydisperse mixture of Table III. Each component is described by a log normal distribution with M_w/M_n = 1.06.

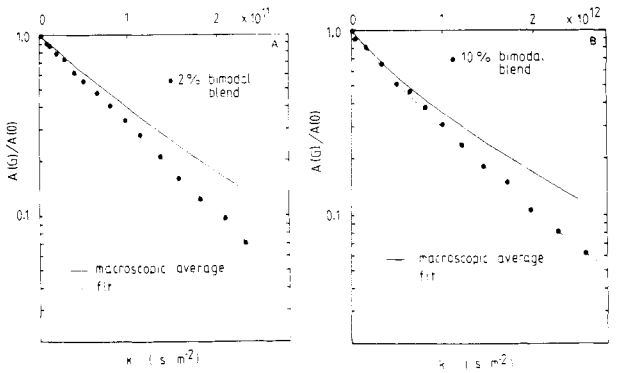

Figure 6. (A) Proton spin-echo attenuation for 2.0% solution of equimolar 110 000 and 233 000 molar mass polystyrene in CCl_4 at 28 °C. The calculated curve labeled "macroscopic average" presumes values of $D_s(M_i)$ pertaining to sharp fraction 2.0% solutions of each component. The curve labeled "fit" uses the actual 110 000 component self-diffusion coefficient obtained from an equivalent solution in which the higher molar mass component was perdeuterated. The fit then reveals the component self-diffusion coefficient of the 233 000 molar mass species. Note that the fit exhibits only slight curvature. Self-diffusion coefficients obtained are given in Table II along with that arising from an averaged single-exponential fit. (B) As for part A but for a 10.0% solution.

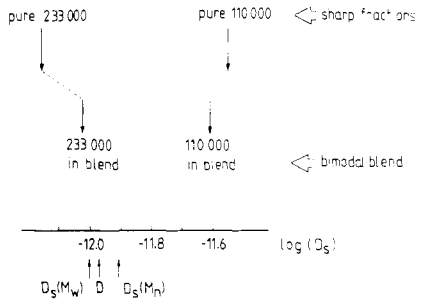

Figure 7. Relative self-diffusion coefficients for sharp fraction and bimodal blend 110 000 and 233 000 molar mass polystyrene solutions at 10.0% concentration. Note the greater shift of the higher molar mass component, consistent with relaxation model based on reptation and tube renewal. The lower arrows give mixture average diffusion coefficients. D corresponds to the single-exponential forced fit while $D_s(M_n)$ and $D_s(M_w)$ are interpolated values corresponding to the indicated mass averages.

bimodal assumption inherent in the following analysis.

The spin-echo attenuation data are shown in Figure 6A,B along with the attenuations calculated by assuming macroscopic averaging alone. It is immediately apparent that although the data are not linear, they are considerably more linear than predicted and hence that considerable ensemble averaging of the respective 110 000 and 233 000 diffusion coefficients has occurred at the microscopic level. Microscopic averaging could be investigated if the diffusion coefficients of the constituents of the blend could be measured. To estimate these diffusion coefficients we have prepared an equimolar blend of protonated 110 000 and perdeuterio 207 000 molar mass polystyrene in carbon tetrachloride. This latter molar mass was the only perdeuterio species available with a molar mass close to a protonated polystyrene suitable for these experiments.

Echo attenuation data were obtained for 110 000 molar mass polystyrene in 110 000/perdeuterio 207 000 equimolar blends at 2.0% and 10.0% concentrations. As expected the data are single exponential since only the protonated polystyrene species (110 000) have been observed. The self-diffusion coefficients obtained are shown in Table II. The changes from the respective values in pure 110 000 molar mass solutions are due to the microscopic averaging which has occurred in the 110 000/207 000 polystyrene blend. These blend values for 110 000 molar mass polymer can now be used to fit the data of Figures 6A,B to determine the self-diffusion coefficients of the 233 000 molar mass components. Here we assume that the diffusion coefficients of the protonated 110 000 molar mass species are not significantly different from those of the 110 000 species in the 110 000/perdeuterio 207 000 equimolar blend. The values so obtained for 233 000 molar mass polystyrene are also given in Table II. It is noteworthy that the fit based on this approach is good. Furthermore, it is ap-

Table III
Composition of Polydisperse Polymer Mixture[a]

polystyrene molar mass	mole fraction
600 000	0.0017
350 000	0.0110
233 000	0.0191
110 000	0.0779
33 000	0.3214
20 400	0.3116
4 000	0.1696
2 000	0.0893

[a] $\langle M_w \rangle = 123500$, $\langle M_n \rangle = 35690$, $\langle M_w \rangle / \langle M_n \rangle = 3.46$.

parent that in both the dilute and semidilute regimes, the larger molar mass has suffered the greatest influence on its diffusive motion when combined in a blend. The relative shifts for the 10% blend are shown in Figure 7. Also shown are the diffusion coefficients of the masses corresponding to the mixture M_n and M_w values along with that derived from a single-exponential fit to the protonated mixture data of Figure 6B. A similar diagram is applicable for the 2% blend. In both solutions the single-exponential fit to the data yields a diffusion coefficient lying between $D_s(M_n)$ and $D_s(M_w)$, the interpolated diffusion coefficients corresponding to M_n and M_w.

We may use the blend data to gain insight into the relative importance of reptation and tube renewal in semidilute chain relaxation. The self-diffusion of a single chain of mass M_1 in a semidilute equimolar blend of M_1 and M_2 may be represented by the relation

$$D_s(M_1) \sim R_1^2\left(\frac{a}{T_r} + b\left[\left(\frac{M_1}{M_1+M_2}\right)\frac{1}{\theta_{r_1}} + \left(\frac{M_2}{M_1+M_2}\right)\frac{1}{\theta_{r_2}}\right]\right) \quad (13a)$$

$$\sim M_1\left(aM_1^{-3} + b\left[\left(\frac{M_1}{M_1+M_2}\right)M_1^{-3} + \left(\frac{M_2}{M_1+M_2}\right)M_2^{-3}\right]\right) \quad (13b)$$

where the factors $M_1/(M_1 + M_2)$ and $M_2/(M_1 + M_2)$ represent the relative weights of topological contraints corresponding to the respective chains. Using eq 13b and the four diffusion coefficients relevant to each blend (see Table II) we are able to independently determine two values of b/a for the blend of 10.0% concentration. The b/a ratios are also given in Table II, where it is apparent that tube renewal is indeed a weak relaxation process. For interest we perform a similar calculation for the 2.0% data, albeit dilute. More experiments involving a greater range of molar masses and concentrations are required to more clearly evaluate this aspect of chain relaxation.

We note that in our work here on bimodal polystyrene samples the average self-diffusion coefficient obtained by fitting the blend echo attenuation to a single exponential falls between those corresponding to the number-averaged and weight-averaged molar masses. We hve made similar measurements on equimass (as opposed to equimolar) blends and find similar results.[4] It is a noticeable trend in these data that the empirical ensemble average diffusion coefficient in fact lies closer to $D_s(M_w)$ than $D_s(M_n)$.

Multimodal Distribution

In order to produce a larger polydispersity we have prepared blends at 2.0% and 10.0% concentrations of polystyrene fractions from 2000 to 598 000 molar mass (see Table III). The calculated number distribution is shown

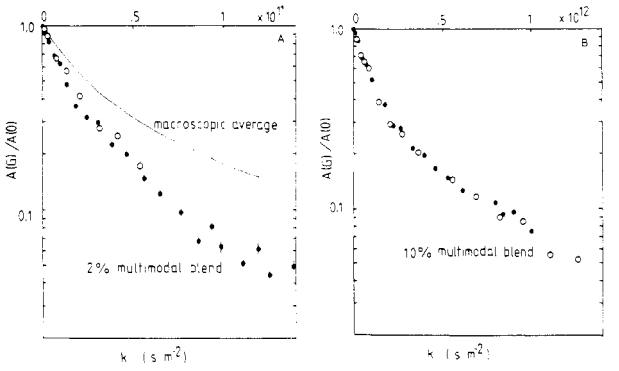

Figure 8. (A) Spin-echo attenuation plot for the highly polydisperse ($M_w/M_n = 1.06$) solution of 2.0% polystyrene in CCl_4. (Open circles Δ = 10 ms, δ = 8 ms; closed circles Δ = 12 ms, δ = 10 ms.) Details of the mixture are given in Table III. The calculated curve presumes $D_s(M_i)$ values pertaining to sharp fractions of the same concentration. The data exhibit microscopic averaging of diffusion coefficients although the range of component values is sufficient to impart a distinct multiexponential behavior. (B) As for part A but for a 10.0% solution. (Open circles Δ = 30 ms, δ = 24 ms; closed circles Δ = 25 ms, δ = 18 ms.)

in Figure 5B. These blends have polydispersities given by $M_w/M_n \simeq 3.5$. The curvature in the PFGNMR spin-echo attenuations is clear in Figure 8A,B. Once again the discrete macroscopic average curves fail to represent the data and in particular overestimate the curvature of the semilogarithmic plots, so it is clear that microscopic averaging is playing a role. In this case however the complexity and wide polydispersity of the blend defy simple analysis.

Curvature in spin-echo attenuation data can arise from restrictions to the diffusive motion as well as from inhomogeneous (multicomponent) motion. A test can however be made that the curvature does result from a sum of Brownian components by varying the diffusive observation time. In Figure 8A,B the data are plotted against $\gamma^2G^2\delta^2(\Delta - \delta/3)$ for different values of $(\Delta - \delta/3)$. Since they fall on common curves, they may be regarded as "well-behaved".

Conclusion

The present work has demonstrated that polydispersities given by $M_w/M_n < 1.10$ present little problem in the interpretation of PFGNMR data and result in single-exponential decays down to an attenuation of at least 0.05 as employed here. This ensemble averaging is predominantly caused by averaging at a microscopic level in which molecular diffusive behavior tends toward a mean diffusion coefficient. Our experiment on bimodal distributions ($M_w/M_n = 1.13$) again illustrates this microscopic averaging and suggests empirically that in sharp fractions the weight-averaged molar mass can best characterize the combined macroscopic and microscopic ensemble average.

Despite the apparent masking of polydispersity effects where M_w/M_n ratios do not exceed 1.10, great care must be taken in testing molar mass dependent scaling laws. As pointed out by Bernard and Noolandi, correlations between polydispersity variations and molar mass can lead to systematic shifts in molar mass scaling exponents. However, these systematic effects are not significant in the experiments of either Leger et al.[8] or ourselves[9,10] on the molar mass dependence of polymer self-diffusion in the semidilute regime and certainly cannot be used to explain the discrepancy between the reported scaling exponents.

It is clear that microscopic averaging in semidilute-solution properties provides insight into the relative importance of reptation and tube renewal in chain relaxation processes. Work is proceeding in which the relative re-

laxation rates are compared in a variety of matrix environments.

Registry No. Polystyrene (homopolymer), 9003-53-6.

References and Notes

(1) Klein, J. *Nature (London)* **1978**, *271*, 143.
(2) von Meerwall, E. *J. Magn. Reson.* **1982**, *50*, 409.
(3) Stejskal, E. O.; Tanner, J. E. *J. Chem. Phys.* **1965**, *42*, 288.
(4) Callaghan, P. T.; Pinder, D. N. *Macromolecules* **1983**, *16*, 968.
(5) Bernard, D. A.; Noolandi, J. *Macromolecules* **1983**, *16*, 548.
(6) Bernard, D. A.; Noolandi, J. *Macromolecules* **1982**, *15*, 1553.
(7) Callaghan, P. T.; Trotter, C. M.; Jolley, K. W. *J. Magn. Reson.* **1980**, *37*, 247.
(8) Leger, L.; Hervet, H.; Rondelez, F. *Macromolecules* **1981**, *14*, 1732.
(9) Callaghan, P. T.; Pinder, D. N. *Macromolecules* **1981**, *14*, 1334.
(10) Callaghan, P. T.; Pinder, D. N. *Macromolecules* **1984**, *17*, 431.

Diffusion Coefficients in Semidilute Solutions Evaluated from Dynamic Light Scattering and Concentration Gradient Measurements as a Function of Solvent Quality. 1. Intermediate Molecular Weights

Wyn Brown* and Robert M. Johnsen

Institute of Physical Chemistry, University of Uppsala, S-751 21 Uppsala, Sweden.

Received April 23, 1984

ABSTRACT: Photon correlation spectroscopy measurements on semidilute solutions of low (10^5) and medium (10^6) molecular weight polystyrene in good (THF, benzene), marginal (ethyl acetate), and Θ (cyclopentane) solvents are described. The autocorrelation function is treated by the cumulant method ($\bar{D}_{cum}$) and by bimodal analysis. In good solvents a main exponent (bimodal analysis) describes a molecular weight independent cooperative diffusion coefficient. A slow component, q^2 dependent, is present in small amount. In ethyl acetate two q^2-dependent modes are present. The relative amplitude of the fast mode (D_C) is strongly concentration and angle dependent. Two modes are also found in the Θ solvent, cyclopentane, again both q^2 dependent. It is concluded that for intermediate molecular weight polymers at semidilute concentrations, dynamic light scattering measurements detect contributions to the dynamic structure factor from two complementary modes: collective motions of the partly-formed pseudogel and center-of-mass translational motions. The classical gradient technique gives values equal to the cooperative diffusion coefficient in a good solvent and to an average of the two modes in a Θ solvent.

Introduction

In dynamic light scattering (QELS) on semidilute polymer solutions there is a now well-documented departure, with increasing concentration (and angle), of the intensity autocorrelation function from a single exponential. In Θ systems, however, the line shape is strongly nonexponential,[1,2,4,10] whereas the effect is less well-pronounced in good solvents.[3,6] For example, when the data are treated by the usual cumulant method, the value of the normalized second cumulant, $\mu_2/\bar{\Gamma}^2$, increases systematically as a function of both concentration and angle. As emphasized by Nose and Chu,[1] this parameter provides a measure of sample polydispersity in dilute solution. In semidilute solutions, however, trends in $\mu_2/\bar{\Gamma}^2$ instead reflect a change in the relative amplitudes of the contributing modes of relaxation. While the predictions of de Gennes' model[11] for semidilute polymer solutions have been invaluable in promoting understanding of the dynamics of transient networks, it becomes increasingly clear that this approach cannot entirely accommodate the observed complexity of the correlation function for intermediate molecular weights. The present contribution is directed toward the elucidation of the interpretation of the nonexponentiality of the spectra as a function of solvent quality and which has caused considerable speculation in the literature. It comprises extensive measurements on narrow fractions of polystyrene of low (10^5) and medium (10^6) molecular weights in good, marginal, and Θ solvents. The QELS data were generally confined to the usually probed $qR_G < 1$ region and in the concentration interval $1 < C/C^* < 10$. In all solvents the angular dependence of the correlation function was examined. The data have been analyzed by both the cumulant method[12] and bimodal analysis. These results are compared with those obtained with the classical macroscopic gradient technique.

Experimental Section

Polystyrenes. Narrow-distribution polymers were purchased from Pressure Chemical Co: PS100, $\bar{M}_w = 93\,000$, $\bar{M}_w/\bar{M}_n = 1.06$; PS300, $\bar{M}_w = 281\,000$, $\bar{M}_w/\bar{M}_n = 1.06$; PS950, $\bar{M}_w = 928\,000$, $\bar{M}_w/\bar{M}_n = 1.06$.

Solvents were spectroscopic grade (Merck, Darmstadt, FRG). The solvents were dried over freshly treated (350 °C, high vacuum) molecular sieves (3 Å, Union Carbide). Earlier measurements had revealed the presence of a slow relaxation in QELS measurements which could be eliminated by thorough drying procedures.

Solutions (QELS) were prepared by weighing. At the high concentrations used here it is not possible to remove extraneous material using centrifugation. Dust-free solutions were prepared by use of a closed-circuit filtration unit. Lower molecular weights (10^5 and 3×10^5) were filtered through 0.22-μm Fluoropore (Millipore) filters and after several hours of repeated filtration, bled off into 10-mm precision-bore NMR tubes. Dilutions were performed by filtering solvent directly into the weighed tubes. In this way a number of optically clear solutions in the range 5–20% (w/w) were prepared in each solvent. At the dilute end of the concentration range, values of the normalized second cumulant ($\mu_2/\bar{\Gamma}^2$) were ≤0.03.

However, with increasing concentration, $\mu_2/\bar{\Gamma}^2$ increased; this parameter also increased with increasing angle at a given concentration (typically in the range 0.03–0.15 as θ increased from 30° to 120°).

With higher molecular weight samples (PS950), 0.5-μm Fluoropore filters were used; otherwise the above-described procedures were employed. Solutions were in each case allowed to stand after

0024-9297/85/2218-0379$01.50/0